

# Title: Implantation Of Engineered Axon Tracts To Bridge Spinal Cord Injury Beyond The Glial Scar In Rats

## Running Head: Engineered Neuronal Scaffolds in Spinal Cord Injury

Patricia Zadnik Sullivan MD, Ahmed AlBayar MD, Justin C. Burrell MS, Kevin D. Browne BA,  
John Arena MD, Victoria Johnson MBChB, PhD, Douglas H. Smith MD, D. Kacy Cullen PhD,  
Ali K. Ozturk MD

### Patricia Zadnik Sullivan, MD

Center for Brain Injury & Repair,  
Department of Neurosurgery,  
Perelman School of Medicine, University of Pennsylvania,  
3400 Spruce St  
Silverstein building, 3<sup>rd</sup> floor  
Philadelphia PA 19104  
215-662-3487  
[Patricia.Zadnik@penmedicine.upenn.edu](mailto:Patricia.Zadnik@penmedicine.upenn.edu)

### Ahmed AlBayar, MD

Center for Brain Injury & Repair,  
Department of Neurosurgery,  
Perelman School of Medicine, University of Pennsylvania,  
3400 Spruce St  
Silverstein building, 3<sup>rd</sup> floor  
Philadelphia PA 19104  
215-662-3487  
[ahmed.albayar@penmedicine.upenn.edu](mailto:ahmed.albayar@penmedicine.upenn.edu)

**Justin C. Burrell, MS**

Center for Neurotrauma, Neurodegeneration & Restoration,  
Corporal Michael J. Crescenz Veterans Affairs Medical Center,  
Philadelphia, PA 19104

215-746-8176

[burrellj@penmedicine.upenn.edu](mailto:burrellj@penmedicine.upenn.edu)

**Kevin D. Browne, BA**

Center for Neurotrauma, Neurodegeneration & Restoration,  
Corporal Michael J. Crescenz Veterans Affairs Medical Center,  
Philadelphia, PA 19104

215-746-8176

[kbrowne@penmedicine.upenn.edu](mailto:kbrowne@penmedicine.upenn.edu)

**John Arena, MD**

Center for Brain Injury & Repair,  
Department of Neurosurgery,  
Perelman School of Medicine, University of Pennsylvania,  
3400 Spruce St  
Silverstein building, 3<sup>rd</sup> floor  
Philadelphia PA 19104

215-662-3487

[John.Arena@penmedicine.upenn.edu](mailto:John.Arena@penmedicine.upenn.edu)

**Victoria Johnson, MBChB, PhD**

Center for Brain Injury & Repair,  
Department of Neurosurgery,  
Perelman School of Medicine, University of Pennsylvania,  
173 Stemmler Hall,  
3450 Hamilton Walk,  
Philadelphia, PA 19104  
215-573-3156  
[vje@pennmedicine.upenn.edu](mailto:vje@pennmedicine.upenn.edu)

**Douglas H. Smith, MD**

Center for Brain Injury & Repair,  
Department of Neurosurgery,  
Perelman School of Medicine, University of Pennsylvania,  
105 Hayden Hall  
3320 Smith Walk  
Philadelphia, PA 19104  
215-573-3156  
[smithdou@pennmedicine.upenn.edu](mailto:smithdou@pennmedicine.upenn.edu)

**D. Kacy Cullen, PhD**

Center for Neurotrauma, Neurodegeneration & Restoration,  
Corporal Michael J. Crescenz Veterans Affairs Medical Center,  
Philadelphia, PA 19104

Center for Brain Injury & Repair,  
Department of Neurosurgery,  
Perelman School of Medicine, University of Pennsylvania,  
105 Hayden Hall  
3320 Smith Walk  
Philadelphia, PA 19104

215-746-8176

[dkacy@pennmedicine.upenn.edu](mailto:dkacy@pennmedicine.upenn.edu)

**Ali K. Ozturk, MD (Corresponding author)**

Center for Brain Injury & Repair,  
Department of Neurosurgery,  
Perelman School of Medicine, University of Pennsylvania,  
3400 Spruce St,  
Silverstein building, 3<sup>rd</sup> floor  
Philadelphia PA 19104

215-662-3487

[ali.ozturk@pennmedicine.upenn.edu](mailto:ali.ozturk@pennmedicine.upenn.edu)

Keywords: Spinal Cord Injury, Tissue Engineering, Bioengineering, Neuroregeneration, Glial Scar, Bioengineered Scaffolds

## Abstract

**Introduction:** Regeneration after spinal cord injury is limited by the presence of a glial scar and inhibitory cell signaling pathways that favor scar formation over re-growth of endogenous neurons. Tissue engineering techniques, including the use of allografted neural networks, have shown promise for nervous system repair in prior studies. Through the use of a minimally invasive injury model in rats, we describe the implantation of micro-tissue engineered neural networks (micro-TENNs) across a region of spinal cord injury, spanning the glial scar to promote axonal regeneration.

**Methods:** Forty-three female Sprague-Dawley rats were included in this study. Micro-TENNs were performed *in vitro* prior to implant, and were comprised of rat sensory dorsal root ganglion (DRG) neurons projecting long bundled axonal tracts within the lumen of a biocompatible hydrogel columnar encasement (1.2 cm long; 701  $\mu\text{m}$  outer diameter x 300  $\mu\text{m}$  inner diameter). Animals were injured using a 2F embolectomy catheter inflated within the epidural space. After a two-week recovery period, micro-TENNs were stereotactically implanted across the injury. Animals were euthanized at 1-week and 1-month after implantation, and tissue was interrogated for the survival of graft DRG neurons and outgrowth of axons.

**Results:** No intraoperative deaths were noted with implantation of the micro-TENNs to span the injury cavity. Graft DRG axons were found to survive at 1-week post-implant within the hydrogel encasement. Graft-derived axonal outgrowth was observed within the spinal cord up to 4.5mm from the implant site at 1-month post-injury. Limited astroglial response was noted within the host, suggesting minimal trauma and scar formation in response to the graft.

**Conclusions:** Micro-TENN sensory neurons survive and extend axons into host spinal cord following a minimally invasive spinal cord injury in rats. This work serves as the foundation for future studies investigating the use of micro-TENNs as a living bridge to promote recovery following spinal cord injury.

## Impact Statement

As spinal cord injury pathology develops, the establishment of a glial scar puts an end to the hope of regeneration and recovery from the consequent neurological deficits. Therefore, growing attention is given to bioengineered scaffolds that can bridge the lesions bordered by this scar tissue. The utilization of longitudinally aligned preformed neural networks – referred to as micro-TENNs – presents a promising opportunity to provide a multi-purpose bridging strategy that may take advantage of several potential mechanisms of host regeneration. In addition to the physical support provided to regenerating spinal cord axons, micro-TENNs also have the potential to provide a functional “cable” that can restore lost connections within the injured spinal cord.

## Introduction

Spinal cord injury (SCI) is a devastating condition most commonly caused by trauma that frequently debilitates the patient with variable degrees of functional loss. Many patients are left with deficits of the motor, sensory and autonomic nervous systems, and chronic issues such as skin breakdown, pain, pneumonia, deep venous thrombosis, and depression frequently ensue. The number of chronic SCI cases in the United States alone has exceeded 275,000 patients<sup>1-3</sup>. The current incidence of new SCI cases in the U.S. is more than 12,000 annually and is expected to rise<sup>2</sup>. Furthermore, the mean age of injury is only 37 years which results in serious social, economic, and psychological impacts on them and their caregivers, and many years of lost productivity<sup>4</sup>.

Despite extensive efforts, SCI remains a difficult problem, mostly due to the hostile environment and limited regenerative capacity of the central nervous system following injury<sup>5</sup>. Clinical experience and *in vivo* animal experiments suggest that there is limited potential for functional recovery after SCI. Neural regeneration following SCI is faced with multiple challenges; principally neuroinflammation<sup>6,7</sup>, inhibitory extracellular matrix (ECM) signals, and reactive astrogliosis resulting in glial scar formation<sup>8,9</sup>.

While damaged axons do form sprouts following injury, these typically will retract following an encounter with the glial scar which is host to a multitude of inhibitory factors. Forming a bridge to span the injury and connecting healthy neural tissue above and below the lesion is, therefore, a logical step to overcome this devastating injury and potentially restore function. Researchers have attempted the implantation of biodegradable scaffolds<sup>10,11</sup>, peripheral nerve grafts<sup>12,13</sup>, embryonal spinal cord grafts<sup>14</sup>, Schwann cells, oligodendrocyte precursor cells, and several types of stem cells<sup>15</sup>. Cell-based therapies have shown promising advantages in terms of local release of neuroprotective factors and focal remyelination, however, they do not promote long-distance regeneration of axonal pathways. On the other hand, while scaffold-based techniques<sup>10,11</sup>, can and do promote axonal regeneration, they lack the biologically supportive environment that neuronal-type or stem cells can provide<sup>16,17</sup>. In these prior studies from our laboratory, stretch-grown constructs were encased within collagen structures to allow handling and implantation of

fragile stretch-grown axons. These early experiments demonstrated successful outgrowth of graft axons into the host spinal cord <sup>16,17</sup>.

Our group has pioneered the development of preformed tissue-engineered living scaffolds that combine cell engineering with advanced biomaterials strategies to generate cellular constructs with a predefined architecture emulating the host nervous system, which unlike acellular approaches, are designed to simultaneously provide structural and trophic support for regenerating axons <sup>18,19</sup>. For CNS repair, we have designed micro-tissue engineered neural networks (micro-TENNs) comprised of two populations of neurons spanned by long axons encased within a protective hydrogel <sup>18-24</sup>. Importantly, micro-TENNs are designed to replicate the systems-level architecture of the CNS defined by discrete neuronal populations spanned by long-projecting axonal tracts, which also resembles the native spinal cord architecture. In addition, the hydrogel encasement protects the transplanted cells from the hostile microenvironment of the injured spinal cord while preserving the preformed neuronal-axonal cytoarchitecture. In turn, the cells are free to interact with the host spinal cord above and below the site of injury, where healthy cell bodies and axons remain. Ideally, the transplanted neurons extend into healthy tissue and promote host axons to cross the site of injury in a process of axon-facilitated axonal regeneration <sup>24</sup>.

In the present study, we investigated the use of micro-TENNs in a rodent model of SCI. The micro-TENN constructs were generated by plating populations of dorsal root ganglia (DRG) neuronal explants tagged with green fluorescent protein (GFP) at both ends of the columnar hydrogel encasement, and an axonal network was allowed to grow *in vitro* to establish a continuous neural bridge. In rats, we employed a minimally invasive model of SCI utilizing an epidural embolectomy balloon catheter to cause mechanical compression <sup>25</sup>. Unlike other models where the spinal cord is transected, an epidural balloon catheter can introduce an injury without an adjacent surgical laminectomy, thus, achieving the desired pathological outcomes without the need to perform clinically irrelevant procedures such as blade-induced or large gap injuries. Further, injury without concomitant decompression allows for maximal isolated injury and more closely reflects

human spinal cord trauma. Animals undergoing epidural compression have shown consistent, durable injury with limited functional recovery<sup>25</sup>.

The goal of this study was to demonstrate the feasibility of using micro-TENNs as a potential living scaffold for SCI repair in a reproducible, clinically relevant epidural compression model while using a minimally invasive implantation technique. Micro-TENN survival and outgrowth into the host spinal cord and the glial scar response post-implantation were characterized histologically. This study provides a foundation for the use of anatomically relevant, biologically active engineered living scaffolds in the treatment of SCI.

### Materials and Methods

All procedures were approved by the University of Pennsylvania's Institutional Animal Care and Use Committee (IACUC) and adhered to the guidelines set forth in the Guide for The Care And Use of Laboratory Animals, Eight edition, 2011 and the Public Health Service Policy on Humane Care and Use of Laboratory Animals (2015). Animals were housed in climate-controlled locations in individually vented rectangular, 131.75 in<sup>2</sup>, 7 inches high, transparent plastic cages. All animals received simple single piece chow and enrichment toys. Animals were house in pairs except in the acute postoperative period to facilitate recovery, drug administration and wound care. Feeding, chow and cages were supervised by the IACUC veterinary care team.

#### *In Vitro Plating of Micro-TENNs*

Micro-TENNs were constructed with an agarose hydrogel outer encasement and extracellular matrix inner lumen (12 mm long, 701  $\mu$ m outer diameter, and 300  $\mu$ m inner diameter) as previously described<sup>22,26,27</sup>. Briefly, the outer hydrogel encasement was generated by drawing molten 3% agarose into a capillary tube (701  $\mu$ m inner diameter). Prior to adding molten agarose, an acupuncture needle (300  $\mu$ m diameter) was inserted into the glass capillary tube to produce the inner lumen. Micro-columns were stored in Dulbecco's phosphate-buffered saline at 4 °C. Micro-columns were UV-sterilized before approximately 25  $\mu$ m of extracellular matrix containing rat tail Type 1 collagen (1.0 mg/ml) and laminin (0.1 mg/ml) in 11.70 mM N-(3-Dimethylaminopropyl)-N'-ethylcarboiimide

10

hydrochloride, 4.3 mM N-Hydroxysuccinimide, and 35.6 mM sodium phosphate monobasic was added to each end of column. Micro-columns polymerized in the incubator for 30 minutes before being rinsed three times with PBS, and then were returned to the incubator overnight.

Dorsal root ganglion (DRG) explants were isolated from E16 rat embryos and stored in Hibernate-E overnight. Cells were transduced with an AAV virus (AAV2/1.hSynapsin.EGFP.WPRE.bGH, University of Pennsylvania Vector Core) to facilitate visualization *in vitro* and *in vivo*. DRG explants were plated on the ends of agarose micro-columns containing crosslinked rat tail Type I collagen similar to previous methodology<sup>26-29</sup>. Micro-TENNs were plated in media consisting of neurobasal containing 10% fetal basal serum conditioned overnight in a flask of spinal astrocytes, supplemented with 37ng/mL hydrocortisone, 2.2 µg/mL isobutylmethylxanthine, 10 ng/mL BDNF, 10 ng/mL CNTF, 10 ng/mL CT-1, 10 ng/mL GDNF, 2% B-27, 20 ng/mL NGF, 20 µM mitotic inhibitors, 2 mM L-glutamine, 417 ng/mL forskolin, 1 mM sodium pyruvate, 0.1 mM mercaptoethanol, 2.5 g/L glucose<sup>30</sup>. Neurite outgrowth was measured via phase microscopy at various days *in vitro* (Figure 1A-E). The mean neurite length at 13 days *in vitro* was 4,398.5 µm ± 302.1 µm with a neurite growth rate of 1,466.2 µm/day ± 100.7 µm/day (mean ± SD; n=6) between days 11 and 13 *in vitro*. At 14 days *in vitro*, micro-TENNs were loaded into a custom-fabricated blunt needle and prepared for implantation (Figure 1A-E). At 14 days *in vitro*, micro-TENNs were loaded into a custom-fabricated blunt needle and prepared for implantation.

#### *Epidural Cord Compression Model*

Animals were anesthetized with 1-5% inhalational isoflurane via a nose cone. Preoperative buprenorphine (0.05mg/kg) and cefazolin were administered (150mg/kg) subcutaneously. The animals were prepped and draped in the usual aseptic fashion. Paw pinch was conducted every 10 minutes to ensure adequate depth of anesthesia.

A 2 cm midline skin incision was made on the dorsal aspect of the lumbar spine centered at L3-4. The L3-4 spinous process and lamina were exposed, and a rongeur was utilized to remove the laminar bone. A 2F Fogarty catheter (Edwards Lifesciences, Irvine CA) was introduced into the epidural space and passed rostrally within the spinal canal 5

cm to the mid-thoracic spine (**Figure 1F, G**). Initial injury characterization was performed to compare partial (50% volume inflation) and complete inflation of the epidural balloon catheter. Eighteen animals were assessed at 1 week (n=4), 2 weeks (n=4), 3 weeks (n=4) and 6 weeks (n=6) with weekly scoring of the BBB. Based on the data from the initial characterization, all animals enrolled in the transplantation cohort received a complete inflation of the balloon catheter and pressure remained constant for 5 minutes. The balloon was then deflated, and the catheter removed from the L3-4 space. After obtaining meticulous hemostasis, the skin was closed with surgical staples. Animals were recovered on heating pads and postoperative buprenorphine (0.05mg/kg) was administered subcutaneously every 8 hours for 24-48 hours in accordance with IACUC recommendations for pain control after SCI procedures. Due to significant motor impairment post injury, Subcutaneous 0.9% normal saline was administered for five days postoperatively to prevent dehydration. Twice daily bladder expression was provided, and animals were observed daily for evidence of complications.

Postoperatively, animal weight, locomotor status, and bladder function were monitored. Restoration of independent bladder emptying was noted for all animals by postoperative day fourteen. There were no intraoperative deaths in this study during the injury and/or transplantation. Animals with greater than 20% weight loss (n=1) or with external signs of physical pain unresponsive to medical therapy were euthanized (n=5). One animal was unenrolled for a defective epidural balloon that failed to deploy. These animals were excluded from the further assessment and analyses.

#### *Stereotactic Injection of Micro-TENN*

Animals underwent a second surgery on day 14-16 post-injury and were randomly enrolled to receive either a micro-TENN (n=11) or acellular micro-column (n=7). The terminal time point for this study were one week (n=4 sensory micro-TENN, n=3 acellular micro-column) or one month (n=7 sensory micro-TENN, n=4 acellular micro-column). Animals were anesthetized as previously described and a 3cm midline dorsal incision was made centered at T7 (defined as the area 5 cm rostral to the L3-4 iliac crest line). A bone rongeur was used to remove the spinous process and lamina at T7 and a myelotomy was

then created using an arachnoid knife at the caudal margin of the spinal cord injury and lateral to the dorsal spinal vein.

The angle of stereotactic injection was customized for each animal. Immediately prior to implantation, the micro-TENN was examined to ensure the viability of the bridging axonal fascicle and to confirm GFP expression. A micro-TENN was loaded into the needle and the internal plunger was withdrawn to the required length. The loaded needle with plunger was then carefully attached to the Hamilton syringe. The Hamilton syringe was then loaded into the stereotaxic arm and advanced into the spinal cord parenchyma along the longitudinal axis of the injury. This allowed the introduction of the micro-TENN to the desired site of implantation across the injury. The needle was then withdrawn (**Figure 1H, I**). A 3mm x 5mm piece of dural matrix was placed over the myelotomy site and the posterior musculature was closed with interrupted 3-0 vicryl suture. The skin was closed with staples, and the animals were recovered on heating pads with frequent monitoring. Postoperative buprenorphine (0.05mg/kg) was administered subcutaneously for the first 24-48 hours and cefazolin (150 mg/kg) was administered daily until resolution of urinary tract infections (commonly lasted up to 5 days) manifested by hematuria or urine cloudiness.

### *Immunohistochemistry*

At the time of euthanasia, animals were anesthetized with an intraperitoneal injection of ketamine/xylazine (100/10 mg/kg) then underwent transcardial perfusion with an initial flush of chilled saline followed immediately by 10% neutral buffered formalin (NBF). Following adequate perfusion, spinal cords were extracted and further post-fixed for 24 hours in NBF at 4°C. Cords were then processed to paraffin using standard techniques. Spinal cords were sectioned axially (8µm-10µm thick) and longitudinally (12 µm thick) using a rotary microtome.

Spinal cords were evaluated with hematoxylin and eosin (H&E) and Luxol Fast Blue/Cresyl Violet (LFB/CV) stains. Additionally, immunohistochemical labeling of spinal cords was performed. Tissue sections were subjected to deparaffinization in xylenes and rehydration to H<sub>2</sub>O through serial ethanol application. Endogenous peroxidase activity was

quenched with immersion in 3% aqueous H<sub>2</sub>O<sub>2</sub> for 15 minutes. Antigen retrieval was achieved with a microwave pressure cooker containing Tris/EDTA buffer. Blocking was performed using normal horse serum (Vector Labs) in Optimax buffer (BioGenex) for 30 minutes followed by incubation in the primary antibody overnight at 4°C. Primary antibodies for DAB peroxidase technique included anti-GFP at 1:40K (Ab290, Abcam), anti-IBA-1 at 1:5000 (234006, Synaptic Systems), anti-GFAP at 1:32K (AB5804, Millipore). After rinsing, sections were incubated in either anti-mouse or anti-rabbit species-specific biotinylated secondary antibody (Vector Labs) at a 1:250 dilution for 30 minutes, followed by the avidin-biotin complex for 30 minutes (Vector Labs). Visualization was achieved using the DAB peroxidase substrate kit (Vector Labs). Sections were counterstained with hematoxylin, followed by rinsing, dehydration, and cover slipped using cyto seal 60. The omission of the primary antibody was performed on injured tissue sections in parallel.

Immunofluorescence IHC technique was performed to further demonstrate the outgrowth of GFP positive axons from the micro-columns. Primary antibodies included rabbit anti-GFP at 1:40K (Ab290, Abcam), goat anti- GFAP at 1:1300 (Ab53554, Abcam), mouse anti-Tuj-1 at 1:1500 (T8578G75, Sigma), chicken anti-IBA-1 at 1:3000 (234006, Synaptic Systems) and Hoechst 33342 at 1:10K (H3570, Invitrogen). After rinsing, secondary antibodies (1:1000 in PBS + 4% NHS) were applied at room temperature for 2 hours (A11057, Invitrogen, red 568 donkey anti-mouse; A21206, Life Technology, green 488 donkey anti rabbit; A21447, Invitrogen, far-red 647 donkey anti-goat; and A11057, Invitrogen, red 568 donkey anti-goat) The sections were fluorescently imaged using a Nikon A1R confocal microscope with 10X air objective and 60X oil objective. For each section, multiple confocal z-stacks were digitally captured and analyzed.

### *Data Acquisition*

All images acquired for comparative analyses were captured with identical acquisition settings. Samples were fluorescently imaged using a Nikon A1Rsi Laser Scanning Confocal microscope with a 20x air or 60x oil objective. Image post-processing and quantification was completed using FIJI (Fiji Is Just ImageJ) software platform<sup>31</sup>. Nikon image files were imported into FIJI via the Bioformats function and each channel was split into individual channels. To minimize potential bias, trained researchers were given only

the axonal channel containing a randomly coded ID. Images were rotated to align the horizontal axis with the inner lumen.

To compare the astrocyte response following transplantation, a macro for automated image processing analyses was designed to minimize any potential bias. For all animals in the longitudinal histological assessment cohort (n=4 micro-TENNs, n=3 acellular), at least two high resolution representative images were taken with the 60x objective at the interface between the micro-column and the injured spinal cord. A 100  $\mu\text{m}$  x 100  $\mu\text{m}$  (length x width) region of interest (ROI) was drawn starting at the edge of the micro-column. Astrocytes were segmented from the GFAP channel using MaxEntropy thresholding and subsequently quantified using the “Analyze Particles” function on features with an area greater than 0.1  $\mu\text{m}^2$  to minimize noisy particles. Mean area percent coverage was calculated by averaging the replicates per animal and then within groups. A log(x+1) data transformation was performed on the mean area percent coverage. Statistical analysis was completed (GraphPad Prism 8 for Windows 64 bit) using two-tailed unpaired Student’s t-tests ( $\alpha = 0.05$ ). Values are reported as mean  $\pm$  SEM.

## Results

### *Sensory Micro-TENN Fabrication In Vitro*

Sensory micro-TENNs were fabricated 1.2-1.4 cm long comprised of discrete populations of sensory neurons from two DRG explants spanned by long axon tracts resembling the neuronal-axonal architecture found in the spinal cord. Micro-TENN neuronal health and neurite outgrowth were assessed during the growth process. Constructs were periodically evaluated qualitatively using phase microscopy to confirm implantation criteria, including healthy neuronal morphology and axons spanning the lumen. The axon growth rate accelerated over the days *in vitro*, yielding a mean growth rate of  $1466.2 \pm 100.7 \mu\text{m}/\text{day}$  between days 11 and 13. At the time of implantation (14 days *in vitro*), micro-TENNs demonstrated healthy neuronal morphology and robust neurite outgrowth (**Figure 1F-I**).

### *Characterization of Epidural Cord Compression Injury*

We sought to explore the injury progression over time in order to aid in the selection of a suitable timepoint for the subsequent micro-TENN implant, based on the extent of injury and stability of the cavitation response. Epidural cord compression injury was characterized at 1, 2, 3, and 6 weeks sacrifice timepoints. For initial characterization in animals that received only the injury, partial inflation resulted in incomplete ambulatory dysfunction postoperatively, with an average BBB score of 11 and complete recovery of hindlimb function by three weeks post-injury (data not shown). In contrast, complete inflation resulted in an average BBB score of 2 post-injury and failed to recover hindlimb function at three weeks (data not shown). These results are consistent with prior studies<sup>25,32,33</sup>. Gross pathological and basic histological assessment demonstrated a consistent gliotic region 8-10 mm in length corresponding to the compression injury (**Figure 2A, B**). Axial sections through the spinal cord demonstrated cavitation rostral to the injury (**Figure 2C-E**) and complete loss of anatomic configuration at the epicenter of the injury (**Figure 2F-H**). Glial fibrillary acidic protein (GFAP) two weeks (**Figure 2C, F, I**) post-injury indicated proliferation and hypertrophy of astrocytes 5mm rostral to the epicenter of injury, consistent with post-injury glial scar formation as previously described<sup>34,35</sup>. IBA-1 staining denoting microglia/macrophage response was noted in sections 5 mm rostral and at the epicenter of injury (**Figure 2D, G, K**). Six weeks post-injury, there was no obvious expansion of the gliotic injury or progressive cavitation on gross histopathological analysis or immunohistochemical investigation beyond a 10mm length.

As an early period with a maximal immune response may be detrimental for transplant cell behavior and survival, two- and three-week post-injury specimens were evaluated to determine an ideal time for implantation to facilitate axon regeneration. Gross pathology at two weeks and three weeks post-injury demonstrated consistent scarring of the spinal cord parenchyma with hemosiderin discoloration and loss of cord volume (**Figure 2A**). Astrocyte proliferation and morphology, indicated by GFAP staining, were comparable in caudal sections obtained two and three-weeks post-injury (**Figure 2I-J**). Microglial activation, noted by the presence of ramified microglia on IBA-1 staining, was similarly consistent in caudal sections at two and three-weeks post-injury (**Figure 2K-L**).

Therefore, the two-week timepoint was selected for post-injury implantation of micro-TENNs.

### *Survival and Outgrowth of Micro-TENN Axons Following Implantation*

All micro-TENNs selected for implant demonstrated positive GFP signal immediately prior to implantation and exhibited robust axon fascicles. Stereotactic implantation was successful in all animals and no intraoperative deaths were observed during micro-TENN (or empty micro-column) implantation.

One week after implantation, GFP/Tuj1+ axons were identified within the lumen of the micro-TENN on axial sections (**Figure 3A-C**) and GFP positive axons seen on DAB staining were present in longitudinal sections indicating that DRG-axons within the micro-TENN survived manipulation and implantation into the spinal cord and retained GFP expression (**Figure 4A-E**).

One month after implantation of micro-TENNs, sections through the region of injury confirmed the trajectory of the micro-TENNs within the spinal cord parenchyma. GFP positive axonal outgrowth into the host spinal cord was visualized extending from the transplanted micro-TENN (**Figure 5A-D**). Positive co-labeling with Tuj-1 and GFP was found with cellular micro-TENN implants following fluorescent immunohistochemistry (**Figure 5E-J**). The greatest distance recorded from the micro-TENN was 4.5 mm rostrally and more than 2 mm caudally into the host spinal cord (**Figure 5E**). These findings suggest that the micro-TENN implant formed a living tissue bridge within the spinal cord.

A limited glial response was observed at 1-month post transplantation at the host-implant interface as evidenced by few astrocytes at the border of the implant with Tuj1 positive axons at the borders of the micro column (**Figure S1**). No statistical differences in the astrocyte coverage at the interface between the micro-column and the host spinal cord tissue was observed between the micro-TENN (9.0 %  $\pm$  6.1 %) and acellular (13.0 %  $\pm$  10.9 %) groups (**Figure 6A-E**).

## Discussion

While there are many reasons that clinically meaningful treatment of SCI has remained elusive, a major area of concern is the poor clinical relevance of many SCI injury models and treatment modalities. Therefore, in this study, we employed a model that produces SCI of similar appearance as found in humans<sup>36</sup>. Specifically, epidural compression injury in the absence of decompressive laminectomy replicates common neuropathological aspects of human SCI lesions. Cavitation was noted up to 6 weeks post-injury, however, the length of this cavity did not expand beyond the implanted micro-TENN length. We then used a minimally invasive method to stereotactically transplant DRG derived sensory neuron micro-TENNS across the SCI lesion cavity. We found micro-TENN survival and outgrowth up to 4.5 mm away from the implant site into the healthy host tissue, rostrally and caudally, at one-month post-implantation. Further, the axon bridge within the hydrogel encasement survived the implantation, bringing the total length of the living tissue bridge to over 2 cm at one-month post-implantation, the endpoint of our study. These findings suggest that micro-TENN implantation may enable host regeneration by bridging the lesion site as an axon-based living scaffold.

Indeed, axonal re-growth to bridge a lesion and the formation of new functional connections following injury is not inherently impossible. Promising efforts thus far can be categorized into cell-based therapies (including stem cells and neural cells) and biomaterial scaffolds. Cell-based therapies have the purported advantage of releasing neurotransmitters and other neuroprotective factors and can be effective in encouraging remyelination while potentially also replenishing lost neural cells. On the other hand, scaffolding techniques serve as a guide for sprouting host axons and can assist in their regrowth across significant distances. Our group has pioneered anatomically inspired micro-tissue engineering techniques to create micro-TENNS, which are miniaturized, transplantable, fully encapsulated constructs comprised of axonal tracts spanning two populations of neurons. As such, micro-TENNS represent a promising strategy to combine the advantageous aspects of both cell-based and biomaterial-based treatment modalities by creating a neural cell-based, living scaffold to aid the regeneration of surviving host axons. In a process akin to CNS development during embryogenesis, transplanted cells may

serve as pioneer axons to the regenerating host axons extending across an injury site<sup>37</sup>. Furthermore, the transplanted and host axons are relatively protected from the surrounding hostile environment in a hydrogel encasing, which has the added benefit of minimizing damage to the cells during surgical implantation.

In these experiments, we used micro-TENNs in a rodent embolectomy balloon-compression SCI model. This method of injury has several advantages, such as the surgical laminectomy needed to insert the catheter is distal to the injury site and subsequent repair efforts, which reduces scar tissue formation and mitigates the need for extensive debridement at the time of implantation. Furthermore, the lack of a decompressive laminectomy at the injury site more closely resembles human cases and may more accurately reflect the cascade of injury following SCI. In keeping with other groups' experiences, the embolectomy balloon compressive injury model produced lasting and reproducible injuries in our experiments. We transplanted micro-TENNs comprised of sensory neurons and pre-formed internal axonal tracts at two weeks following injury to allow for the initial inflammatory response to abate in intensity and for a stable lesion to have formed.

Our results at one-week post-implantation show that the transplanted DRG axons via micro-TENNs survive in the host spinal cord and maintain their cytoarchitecture within the hydrogel encasement. Furthermore, at one-month post-transplant, we have shown that transplanted axons extend up to 4.5 mm in the host spinal cord rostrally and up to 2 mm caudally. Implant-derived GFP-positive axons were confirmed via DAB and Tuj1/GFP colocalization in longitudinal spinal cord sections one-month following micro-TENN implantation. We believe this has important implications in the treatment of SCI as axons bridging the entirety of an injury site and extending past the glial scar may form the framework upon which host axons can regenerate and reestablish functional connections. At one month post-implantation, the presence of both surviving luminal axons and axons extending into the host parenchyma support the idea of the micro-TENN as a type of node in the spinal cord neuronal network, acting as a conduit to restore connectivity rostral and caudal to the region of SCI. Further, along the tract of the micro-TENN implant, a limited glial response was seen. Notably, there was no difference in the astrocyte response

between the micro-TENN and the acellular control, suggesting the exogenous cells did not exacerbate a glial scar response around the construct. Progressive cavitation around the implant was not observed one-month post-implantation, further highlighting the incorporation of grafts into a host without significant inflammatory reactions, tissue necrosis, or reactive astrogliosis.

In this study, our objective was to demonstrate the feasibility of utilizing micro-TENNs as regenerative strategy to bridge an injury cavity in a reproducible, clinically relevant epidural spinal cord compression model. We found micro-TENN neuronal survival and axonal outgrowth into the host spinal cord with minimal glial scar response surrounding the construct. Moreover, regenerating host axons were found in close proximity spanning the interface of the injury site, suggesting that micro-TENNs may serve as a living scaffold for regenerating axons. This work provides a foundation for the use of anatomically relevant, biologically active engineered living scaffolds in the treatment of SCI. However, while our goal in this study was to demonstrate feasibility, future studies will be required to assess whether implanted micro-TENNs result in improved functional recovery. Indeed, a limitation in the current study was the lack of functional assessment and detailed measurements of host axon regeneration, in context with measures of micro-TENN survival and outgrowth. If necessary, additional future work may include optimization studies to improve the consistency of micro-TENN outgrowth, including alternative bioencasements and/or cell sources. Host axon regeneration may be evaluated using anterograde tract tracing to investigate whether host axons are regenerating across the micro-TENN, thus utilizing the construct as a bridge to encourage the growth of new axonal tracts. Following optimization, researchers will be well-positioned to investigate whether micro-TENN transplantation improves functional recovery following SCI. Here, daily physical rehabilitation may be necessary to maintain limb flexibility and electrophysiological studies will be required to assess for functional connectivity following micro-TENN implantation.

## Conclusion

Micro-TENNs are a promising regenerative strategy for SCI designed for minimally invasive implantation. Herein, we show methodology for minimally invasive injury and

surgical implant, along with evidence of micro-TENN neuronal survival, axonal outgrowth, and structural integration with the host spinal cord in a rodent model of SCI. As an axon-based living scaffold, micro-TENNs may promote host corticospinal regeneration or act a functional relay across the damaged segment; however, future work is necessary to elucidate underlying mechanisms and implications for functional recovery.

### **Acknowledgments**

Financial support was provided by the U.S. Department of Defense [CDMRP/JPC8 W81XWH-16-1-0796 (D.K.C)], the Department of Veterans Affairs [BLR&D Merit Review I01-BX003748 (D.K.C)], and the National Institutes of Health [U01-NS094340 (D.K.C) and R01-NS043126 (D.H.S)].

### **Authors' disclosure**

D.K.C. and D.H.S. are scientific co-founders of Innervace, Inc., and Axonova Medical, LLC, which are University of Pennsylvania spin-out companies focused in neuroregenerative medicine. Multiple patents relate to the composition, methods, and use of micro-tissue engineered neural networks, including U.S. Patent App. 15/032,677 (D.K.C and D.H.S) and U.S. Patent App. 16/093,036 (D.K.C and D.H.S). The remaining authors do not declare any commercial or financial relationships that could be construed as a potential conflict of interest.

## References:

1. Lasfargues, J.E., Custis, D., Morrone, F., Cars well, J., and Nguyen, T. A model for estimating spinal cord injury prevalence in the United States. *Spinal Cord* . Nature Publishing Group, **33**, 62, 1995
2. Majdan, M., Brazinova, A., and Mauritz, W. Epidemiology of traumatic spinal cord injuries in Austria 2002–2012. *Eur Spine J* . Springer Berlin Heidelberg, **25**, 62, 2016
3. DeVivo, M.J., and Chen, Y. Trends in New Injuries, Prevalent Cases, and Aging With Spinal Cord Injury. *Arch Phys Med Rehabil* . W.B. Saunders, **92**, 332, 2011
4. Singh, A., Tetreault, L., Kalsi-Ryan, S., Nouri, A., and Fehlings, M.G. Global Prevalence and incidence of traumatic spinal cord injury. *Clin. Epidemiol.* Dove Medical Press Ltd, pp. 309–31, 2014.
5. Anderson, M.A., O’Shea, T.M., Burda, J.E., Ao, Y., Barlatey, S.L., Bernstein, A.M., et al. Required growth facilitators propel axon regeneration across complete spinal cord injury. *Nature*. Nature Publishing Group, pp. 396–400, 2018.
6. Rust, R., and Kaiser, J. Insights into the Dual Role of Inflammation after Spinal Cord Injury. *J Neurosci* . Society for Neuroscience, **37**, 4658, 2017
7. Anwar, M.A., Al Shehabi, T.S., and Eid, A.H. Inflammogenesis of Secondary Spinal Cord Injury. *Front Cell Neurosci* . Frontiers, **10**, 98, 2016
8. Okada, S., Hara, M., Kobayakawa, K., Matsumoto, Y., and Nakashima, Y. Astrocyte reactivity and astrogliosis after spinal cord injury. *Neurosci Res* . Elsevier, **126**, 39, 2018
9. Dyck, S.M., and Karimi-Abdolrezaee, S. Role of chondroitin sulfate proteoglycan signaling in regulating neuroinflammation following spinal cord injury. *Neural Regen Res* . Wolters Kluwer -- Medknow Publications, **13**, 2080, 2018
10. Gros, T., Sakamoto, J.S., Blesch, A., Havton, L.A., and Tuszynski, M.H. Regeneration of long-tract axons through sites of spinal cord injury using templated agarose scaffolds. *Biomaterials* . Elsevier, **31**, 6719, 2010

11. Stokols, S., and Tuszynski, M.H. The fabrication and characterization of linearly oriented nerve guidance scaffolds for spinal cord injury. *Biomaterials* . Elsevier, **25**, 5839, 2004
12. Davies, S.J., Goucher, D.R., Doller, C., Silver, J., Connors, T., Lemay, M.A., et al. Robust regeneration of adult sensory axons in degenerating white matter of the adult rat spinal cord. *J Neurosci* . Society for Neuroscience, **19**, 5810, 1999
13. Levi, A.D.O., Dancausse, H., Li, X., Duncan, S., Horkey, L., and Oliviera, M. Peripheral nerve grafts promoting central nervous system regeneration after spinal cord injury in the primate. *J Neurosurg* . **96**, 197, 2002
14. Kawaguchi, S., Iseda, T., and Nishio, T. Effects of an embryonic repair graft on recovery from spinal cord injury. *Prog Brain Res* . Elsevier, **143**, 155, 2004
15. Assinck, P., Duncan, G.J., Hilton, B.J., Plemel, J.R., and Tetzlaff, W. Cell transplantation therapy for spinal cord injury. *Nat Neurosci* . **20**, 637, 2017
16. Iwata, A., Browne, K.D., Pfister, B.J., Gruner, J.A., and Smith, D.H. Long-term survival and outgrowth of mechanically engineered nervous tissue constructs implanted into spinal cord lesions. *Tissue Eng* . **12**, 101, 2006
17. Ezra Sadik, M., Ozturk, A.K., Albayar, A., Branche, M., Zadnik Sullivan, P., Schlosser, L.O., et al. A Strategy Toward Bridging a Complete Spinal Cord Lesion Using Stretch-Grown Axons. *Tissue Eng Part A* . Mary Ann Liebert Inc, ten. tea.2019.0230, 2020
18. Struzyna, L.A., Harris, J.P., Katiyar, K.S., Chen, H.I., and Cullen, D.K. Restoring nervous system structure and function using tissue engineered living scaffolds. *Neural Regen Res* . Wolters Kluwer -- Medknow Publications, **10**, 679, 2015
19. Struzyna, L.A., Katiyar, K., and Cullen, D.K. Living scaffolds for neuroregeneration. *Curr Opin Solid State Mater Sci* . Elsevier, **18**, 308, 2014
20. Struzyna, L.A., Browne, K.D., Brodник, Z.D., Burrell, J.C., Harris, J.P., Chen, H.I., et al. Tissue engineered nigrostriatal pathway for treatment of Parkinson's disease. *J Tissue Eng Regen Med* . John Wiley & Sons, Ltd, **12**, 1702, 2018

21. Struzyna, L.A., Wolf, J.A., Mietus, C.J., Adewole, D.O., Chen, H.I., Smith, D.H., et al. Rebuilding Brain Circuitry with Living Micro-Tissue Engineered Neural Networks. *Tissue Eng Part A* . Mary Ann Liebert, Inc. 140 Huguenot Street, 3rd Floor New Rochelle, NY 10801 USA , **21**, 2744, 2015
22. Struzyna, L.A., Adewole, D.O., Gordián-Vélez, W.J., Grovola, M.R., Burrell, J.C., Katiyar, K.S., et al. Anatomically Inspired Three-dimensional Micro-tissue Engineered Neural Networks for Nervous System Reconstruction, Modulation, and Modeling Anatomically Inspired Three-dimensional Micro-tissue Engineered Neural Networks for Nervous System Reconstruction, Modulation, and Modeling. Video Link. *J Vis Exp* . **55609379155609**, 2017
23. Cullen, D.K., Tang-Schomer, M.D., Struzyna, L.A., Patel, A.R., Johnson, V.E., Wolf, J.A., et al. Microtissue Engineered Constructs with Living Axons for Targeted Nervous System Reconstruction. *Tissue Eng Part A* . Mary Ann Liebert, Inc. 140 Huguenot Street, 3rd Floor New Rochelle, NY 10801 USA , **18**, 2280, 2012
24. Adewole, D.O., Struzyna, L.A., Harris, J.P., Nemes, A.D., Burrell, J.C., Petrov, D., et al. Optically-Controlled “Living Electrodes” with Long-Projecting Axon Tracts for a Synaptic Brain-Machine Interface. *SSRN Electron J* . Elsevier BV, 2018
25. Vanický, I., Urdzíková, L., Saganová, K., Cízková, D., and Gálik, J. A simple and reproducible model of spinal cord injury induced by epidural balloon inflation in the rat. *J Neurotrauma* . Mary Ann Liebert, Inc., **18**, 1399, 2001
26. Struzyna, L.A., Harris, J.P., Katiyar, K.S., Isaac Chen, H., and Kacy Cullen, D. Restoring nervous system structure and function using tissue engineered living scaffolds. *Neural Regen Res*. Editorial Board of Neural Regeneration Research, **10**, 679, 2015.
27. Harris, J.P., Struzyna, L.A., Murphy, P.L., Adewole, D.O., Kuo, E., and Cullen, D.K. Advanced biomaterial strategies to transplant preformed micro-tissue engineered neural networks into the brain. *J Neural Eng*. Institute of Physics Publishing, **13**, 2016.

28. Adewole, D.O., Struzyna, L.A., Harris, J.P., Nemes, A.D., Burrell, J.C., Petrov, D., et al. Optically-Controlled “Living Electrodes” with Long-Projecting Axon Tracts for a Synaptic Brain-Machine Interface. *bioRxiv*. Cold Spring Harbor Laboratory, 333526, 2018.
29. Hou, S., Tom, V.J., Graham, L., Lu, P., and Blesch, A. Partial restoration of cardiovascular function by embryonic neural stem cell grafts after complete spinal cord transection. *J Neurosci* . **33**, 17138, 2013
30. Katiyar, K.S., Struzyna, L.A., Das, S., and Cullen, D.K. Stretch growth of motor axons in custom mechanobioreactors to generate long-projecting axonal constructs. *J Tissue Eng Regen Med* . John Wiley and Sons Ltd, **13**, 2040, 2019
31. Schindelin, J., Arganda-Carreras, I., Frise, E., Kaynig, V., Longair, M., Pietzsch, T., et al. Fiji: An open-source platform for biological-image analysis. *Nat. Methods*. 2012.
32. Su, Y.F., Lin, C.L., Lee, K.S., Tsai, T.H., Wu, S.C., Hwang, S.L., et al. A modified compression model of spinal cord injury in rats: Functional assessment and the expression of nitric oxide synthases. *Spinal Cord*. Nature Publishing Group, **53**, 432, 2015.
33. Khan, M., and Griebel, R. Acute spinal cord injury in the rat: Comparison of three experimental techniques. *Can J Neurol Sci / J Can des Sci Neurol* . Cambridge University Press, **10**, 161, 1983
34. Göritz, C., Dias, D.O., Tomilin, N., Barbacid, M., Shupliakov, O., and Frisén, J. A pericyte origin of spinal cord scar tissue. *Science (80- )*. **333**, 238, 2011.
35. Soderblom, C., Luo, X., Blumenthal, E., Bray, E., Lyapichev, K., Ramos, J., et al. Perivascular fibroblasts form the fibrotic scar after contusive spinal cord injury. *J Neurosci*. **33**, 13882, 2013.
36. Norenberg, M.D., Smith, J., and Marcillo, A. The Pathology of Human Spinal Cord Injury: Defining the Problems . *J. Neurotrauma*. 2004.

37. Katiyar, K.S., Struzyna, L.A., Morand, J.P., Burrell, J.C., Clements, B., Laimo, F.A., et al. Tissue Engineered Axon Tracts Serve as Living Scaffolds to Accelerate Axonal Regeneration and Functional Recovery Following Peripheral Nerve Injury in Rats. bioRxiv . Cold Spring Harbor Laboratory, 654723, 2019

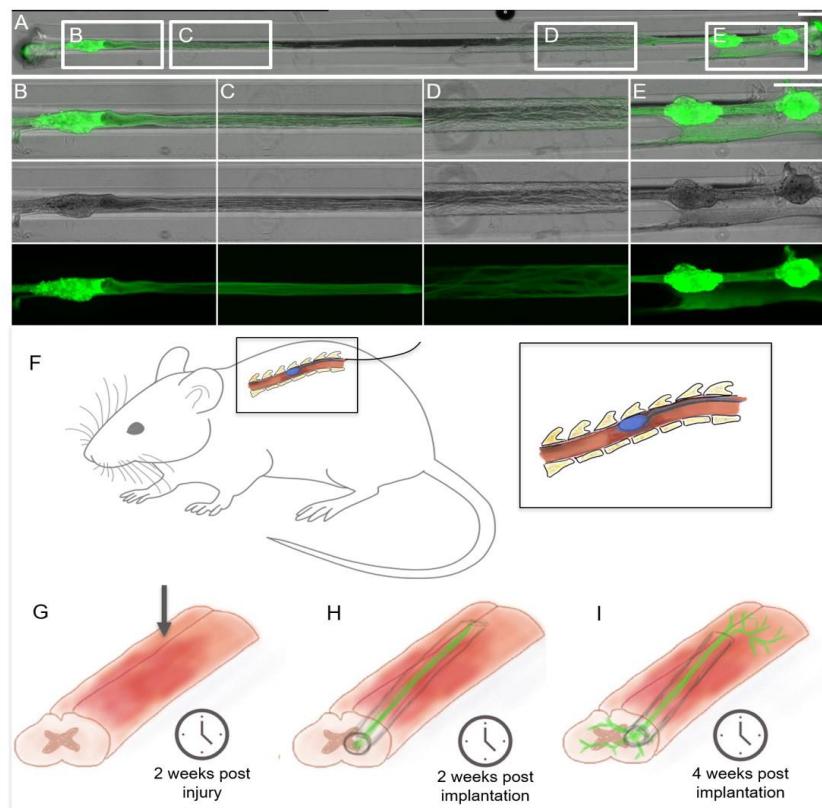


**Figure 1. Micro-TENN fabrication at 14 Days *in vitro* and experimental design and concept.** (A) Micro-TENNs were fabricated by loading DRG explants on either end of a 12.4 mm long agarose micro-column prefilled with ECM. DRG explants were transduced with GFP to facilitate visualization. Prior to implantation, micro-TENNs were imaged at 14DIV to confirm neuronal health, axonal outgrowth, and positive fluorescence using phase and epifluorescent microscopy. (B-E) At higher magnification, discrete populations of GFP+ neurons spanned by long axons within the lumen of the micro-column were visualized. Scale bar: 500  $\mu\text{m}$ . (F-I) A schematic of the balloon compression procedure and micro-TENN transplantation is shown. (F) Female Sprague Dawley adult rats were injured using an epidural balloon that was introduced via laminectomy at L3-4 and passed to the mid-thoracic spine. It was inflated to induce spinal cord injury at mid-thoracic spine (inset). (G) Two weeks after injury, a laminectomy was performed 5cm rostral to L3-4 and a myelotomy was performed (arrow). (H) The micro-TENN was then injected using a stereotactic needle within the spinal cord parenchyma. (I) Four weeks later, axons were visible extending in the surrounding spinal cord parenchyma. DRG: Dorsal Root Ganglia, ECM: Extracellular Matrix, GFP: Green Fluorescent Protein, DIV: Days *In Vitro*.

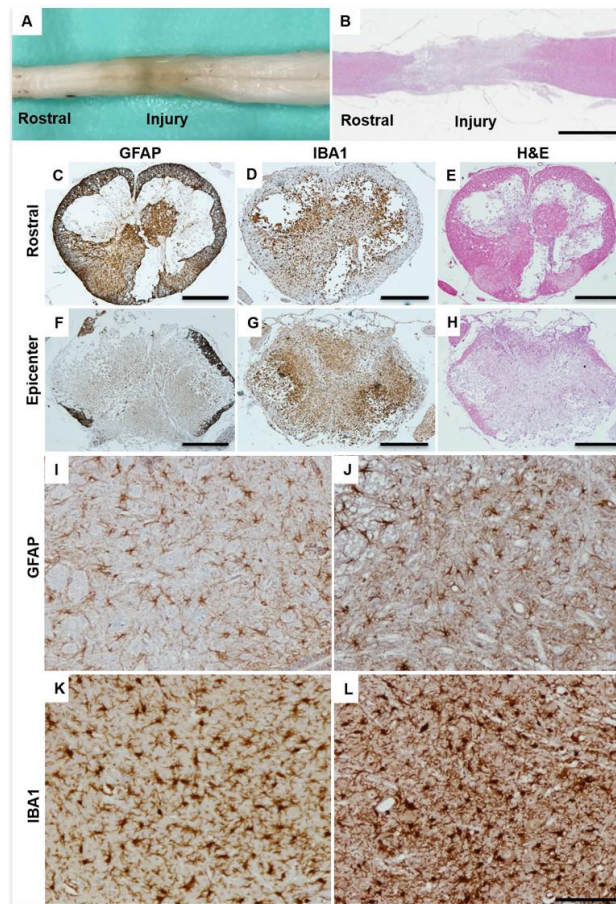


**Figure 2. Gross pathology and immunohistochemistry of injured animals at two- and three weeks post-injury.** (A) A gross specimen at two weeks post-injury. (B) H&E staining demonstrating the injured area. Scale bar: 3mm. (C-H) axial sections representing pathology 2 weeks post-injury. Scale bars: 1000 $\mu$ m. GFAP staining at 5mm rostral to injury (C) and at the epicenter of the injury (F). IBA-1 staining 5mm rostral (D) and at the epicenter of injury (G). H&E staining at 5mm rostral (E) and at the epicenter of injury (H). (I-J) GFAP staining of gray matter in axial spinal cord sections taken 5mm caudal to injury indicate similar astrocyte morphology and proliferation at two weeks (I) and three weeks (J) post-injury. (K-L) IBA-1 staining demonstrating comparable number and morphology of ramified microglia in sections 5mm caudal to the injury at two weeks (K) and three weeks (L) post-injury. Scale bars: 100 $\mu$ m. IBA-1: ionized calcium-binding adaptor molecule 1, GFAP: glial fibrillary acidic protein.

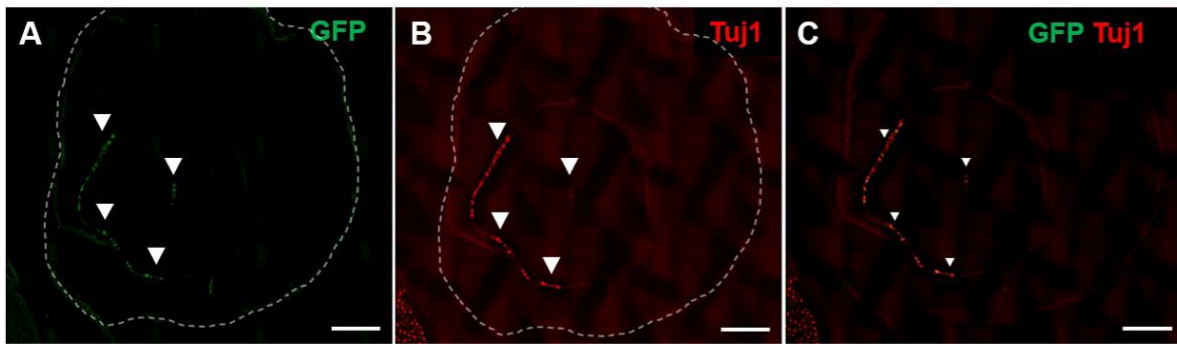


**Figure 3. Axial sections of the injured spinal cords at the epicenter at one- week post-implantation.** The outer lumen of the micro-TENN is illustrated by the dashed line in (A, B) (A) Tuj1 positive staining indicative of axons (arrowheads) along the inner lumen of the micro-TENN. (B) GFP positive staining indicative of implant-derived DRG neurons within the lumen of the micro-TENN. (C) Co-localization of Tuj1 and GFP positive axons within the inner lumen of the micro-TENN. Scale bar 100 $\mu$ m. GFP: green fluorescent protein, Tuj1: neuron-specific class III $\beta$  tubulin.

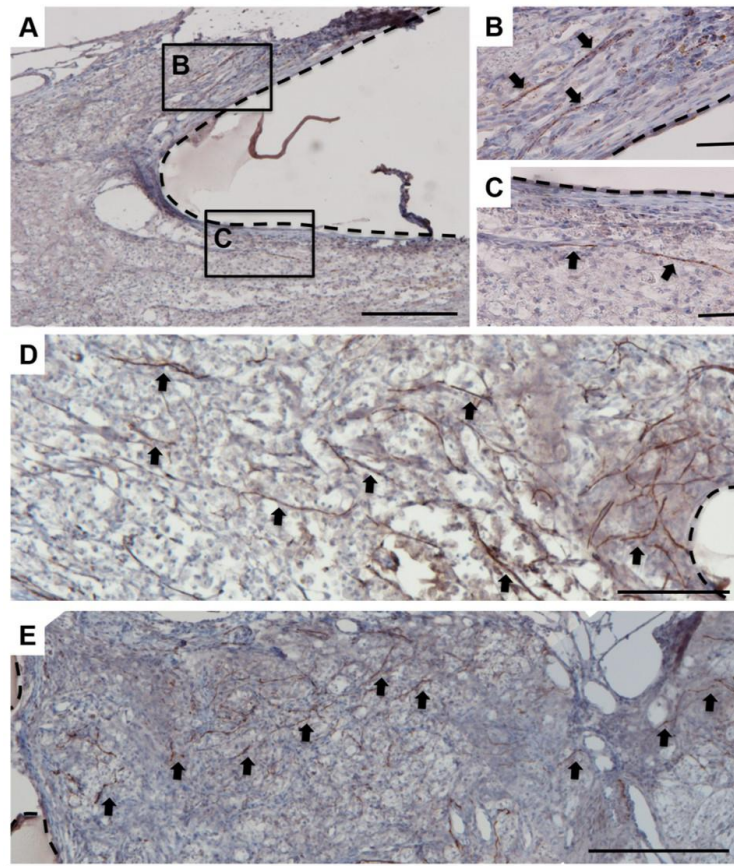


**Figure 4. DAB (3,3'-Diaminobenzidine) Immunohistochemistry demonstrating GFP positive axons in longitudinal spinal cord sections one month after micro-TENN implants.** Micro-TENN lumen marked with black dashed line. (A) Rostral spinal cord section with visible micro-TENN lumen. Scale bar: 250 $\mu$ m. Inset (B) and (C) with brown axons indicated with black arrows. Scale bar: 50 $\mu$ m. (D) Caudal spinal cord with axons (black arrows) extending along the background of necrotic injured tissue. Scale bar: 250 $\mu$ m. (E) Rostral spinal cord with axons extending longitudinally (black arrows). Scale bar: 500 $\mu$ m.

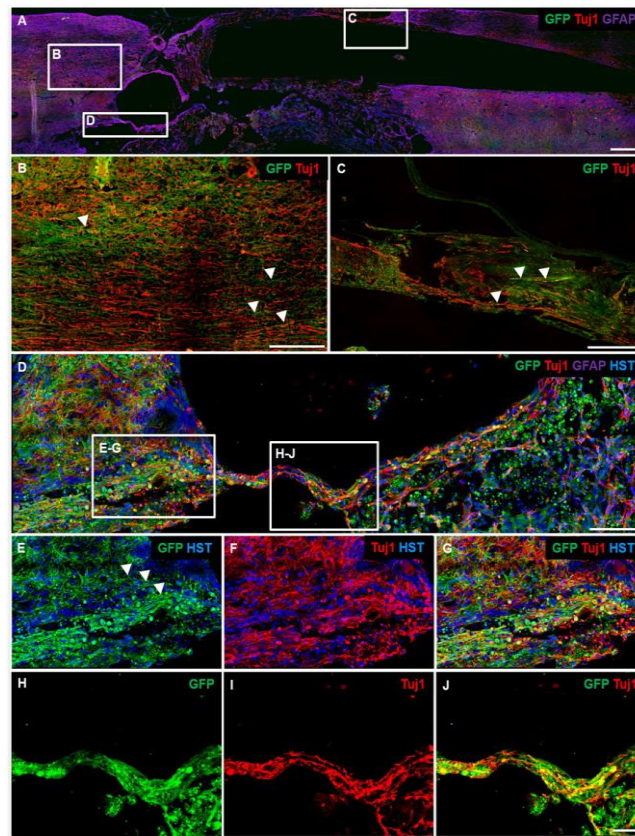


**Figure 5. Longitudinal section of an injured spinal cord at 1-month post-implantation demonstrating micro-TENN axonal extension and host axon regeneration.** At 1-month post-repair, a longitudinal section revealed the micro-TENN spanning the dorsal and caudal aspects of the injured spinal cord. Fluorescent labeling was completed to enable visualization of micro-TENN neurons/axons (GFP), neurons/axons (Tuj1), and astrocytes (GFAP). Significant damage to the nervous tissue architecture was readily apparent across the entire injury site across all animals at 1-month post repair (6 weeks post-injury). Scale bar: 1000 $\mu$ m. (B, C) At higher magnification, micro-TENN axons were found extending into the host spinal cord. Arrowheads denote co-localization of GFP and Tuj1. Scale bar: 250 $\mu$ m. (D) Inset of the rostral interface showing successful structural integration of the micro-TENN with the host spinal cord outside the injury site at 1-month post-implantation. Scale bar: 100  $\mu$ m. (E-G) At high magnification, robust micro-TENN outgrowth was visualized extending into native host spinal cord tissue. Scale bar: 100  $\mu$ m. (H-J) At the edge of the interface, a dense region of micro-TENN axons was found spanning the injury site that connected the micro-TENN to the host spinal cord tissue. Notably, host axons (GFP-, Tuj1+) were observed extending from the native host spinal cord in close proximity

to the axonal outgrowth from the micro-TENN (GFP+, Tuj1+). These findings indicate micro-TENNs may serve as a living scaffold for regenerating host axons. Scale bar: 100  $\mu$ m. HST: Hoechst nuclear staining, GFAP: Glial fibrillary acidic protein, GFP: green fluorescent protein, Tuj1: neuron-specific class III $\beta$  tubulin.

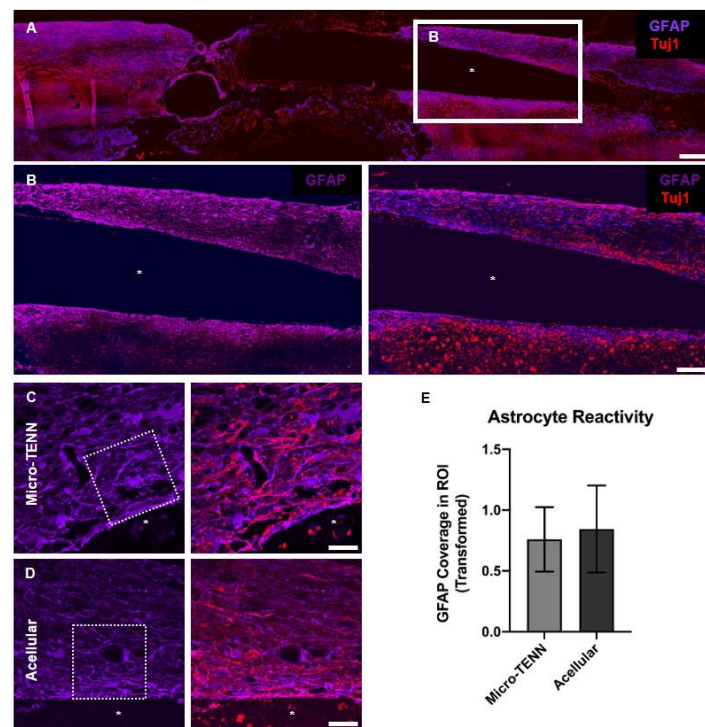


**Figure 6. Comparison of astrocyte response around the micro-column at 1-month post-implantation.** Longitudinal spinal cords at 1-month post-implantation were sectioned and stained to identify astrocytes (GFAP) and neurons/axons (Tuj1). The agarose micro-column is denoted by the asterisk. (A) A representative image at low magnification showing elevated glial response at the border of the spinal cord injury with minimal response surrounding the micro-column and an absence of axons coursing throughout the injury were observed, as expected following SCI. Scale bar: 1000  $\mu\text{m}$ . (B) At higher magnification, minimal astrocytic response was visualized surrounding the lumen of the micro-column. Host neurons were also found in close proximity to the micro-column, suggesting these neurons survived the initial SCI as well as the micro-TENN implantation. Scale bar: 250  $\mu\text{m}$ . (C, D) Insets at higher magnification of areas surrounding micro-TENNs implantation site, regions of interest for GFAP signal comparison is outlined with dotted squares (100  $\mu\text{m}$  x 100  $\mu\text{m}$ ). (E) Mean area percent coverage comparison of averaged 2 replicates per animal in each group (micro-TENNs implantation; n=4 and acellular control group; n=3) at 1-month timepoint using a two-tailed students' t test. GFAP: Glial fibrillary acidic protein, GFP: green fluorescent protein, Tuj1: neuron-specific class III $\beta$  tubulin.